

The Granite III upgrade program of the Whipple Observatory

J. P. Finley¹ and the VERITAS collaboration²

¹Dept. of Physics, Purdue University, 1396 Physics Building West Lafayette, IN 47907

²Fred Lawrence Whipple Observatory, Harvard-Smithsonian CfA, PO Box 97, Amado, AZ, 85645, USA

Abstract. The Whipple collaboration completed its GRANITE III upgrade program during the 1999–2000 observing seasons. The final phase of the program was installation of a small pixel camera with the aim of increasing the sensitivity of the Whipple 10 meter telescope and, simultaneously, reducing the energy threshold of the instrument. We report on the results of the upgrade and specifically will describe the results for the small pixel camera.

1 Introduction

The field of Very High Energy (VHE) gamma-ray astronomy has seen rapid growth over the past 10 years and several classes of VHE sources have been catalogued; for a recent review of the field see Catanese and Weekes (1999). The progress was in large part due to the development of the imaging atmospheric Cherenkov technique that was pioneered by the Whipple collaboration using the 10m telescope located at the Fred Lawrence Whipple Observatory in southern Arizona. Over the past decade the focal plane cameras in use at the existing VHE observatories have progressively been expanded in both field-of-view and pixelization with the aim of increasing the sensitivity of the telescopes to gamma-rays and, simultaneously, reducing the threshold energy of the instruments. The Whipple collaboration carried out a program to upgrade the focal plane detector of the 10m telescope, dubbed the GRANITE III upgrade, which, starting in 1996, lasted 3 years. There were 3 distinct phases of the upgrade: (1) commissioning of a large field-of-view camera ($\sim 5^\circ$ diameter) with $0^\circ.25$ pixels, (2) commissioning of a hardware pattern recognition trigger, and finally (3) the installation and commissioning of a small pixel, high resolution camera ($\sim 0^\circ.12$ center-to-center pixel spacing). Phase (1) was carried out during the summer and fall of 1997 while phase (2) was completed during the winter of 1998. The results of those two components of the upgrade have been re-

ported elsewhere (Finley et al., 2000). The final phase of the upgrade, the installation and commissioning of the high resolution camera, was carried out during the summer and fall of 1999. Additionally the individual mirror facets of the 10m reflector were realuminized during the 1999–2000 observing season. In this article we describe the final phase of the upgrade and present results demonstrating its performance.

2 The GRANITE III 490 Pixel Camera

During the summer and fall of 1999 a 490 pixel high resolution camera was installed at the Whipple observatory. The camera consists of 379 13mm PMTs (Hamamatsu model #H3165 consisting of an R960 PMT and a passive resistive divider chain) constituting a $2^\circ.6$ diameter inner camera surrounded by 111 28mm PMTs (Hamamatsu model #R1398) which fills out the field-of-view to $4^\circ.0$ diameter. The system is triggered on light collected in the innermost 331 pixels. A picture of the camera in place at the focal plane of the 10m telescope is displayed in Figure 1. The center-to-center spacing of the inner pixels is $\sim 0^\circ.12$ in the 10m focal plane while the outer pixels are spaced at $\sim 0^\circ.24$ but in a circular rather than close packed arrangement. The outer rings of 28mm PMTs utilize analog fiber optic links to transmit their signals from the telescope to the electronics area. A complete description of the analog fiber optic links and their performance can be found in De La Calle Perez et al. (2001). A simple set of light concentrators are installed on the inner 379 pixels to reduce the amount of dead space between the individual channels. The concentrators are overlapping truncated cones machined from a single piece of $1/2''$ thick polycarbonate. These are flame polished and aluminized by vacuum evaporation. The concentrators provide an increase of $\sim 38\%$ in the amount of light collected by the camera. The installation of the high resolution camera was carried out during the summer of 1999 and first light was achieved in the early fall of 1999.

During 1999 and 2000 the individual mirror facets were re-

Correspondence to: J. P. Finley (finley@physics.purdue.edu)

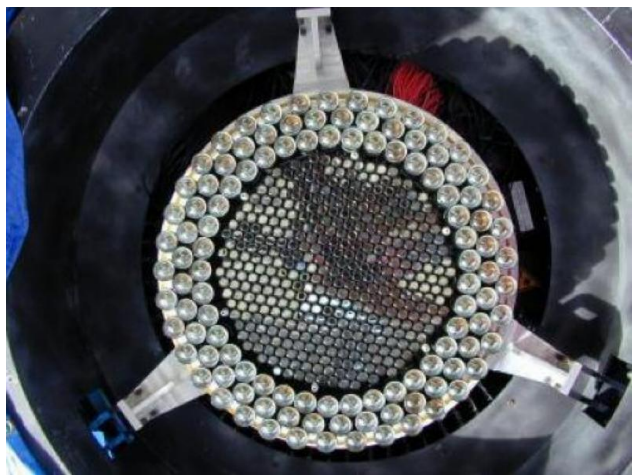


Fig. 1. The GRANITE III 490 pixel camera in the focal plane of the Whipple observatory 10m telescope. The light concentrator plate has been removed in this image.

coated to improve the light gathering capabilities of the 10m reflector. The entire complement of mirrors for the 10m reflector takes on the order of 1 year to recoat so the 10m was operated with typically 20 individual facets removed at any given time during the 1999–2000 observing season so that the scientific program could proceed uninterrupted. A detailed description of the mirrors and the coating procedures can be found in Badran (2001).

The GRANITE III upgrade, including the mirror recoating, was thus completed in the summer of 2000 and the 2000–2001 observing season was the first with the fully upgraded system.

3 Performance of the High Resolution Camera

The Crab Nebula is the standard candle of VHE gamma-ray astronomy (Weekes et al., 1989) and of many other branches of high energy astronomy. The Crab Nebula is routinely monitored with the 10m telescope for normalization of the instrumental response from season to season as changes and improvements are made to the system. The hardware triggering level of the individual pixels is a priori determined by taking a bias curve with the telescope pointing at a dark sky field and varying the downstream discriminators as displayed in Figure 2. There are 2 distinct components of the bias curve; triggers resulting from night sky coincidences (the steep curve at low discriminator settings in Figure 2), and triggers due to cosmic ray initiated events (the flat curve at higher discriminator settings). The hardware pattern recognition trigger suppresses the night sky initiated events relative to a simple multiplicity trigger and allows for a lower hardware threshold (Bradbury and Rose, 2001). Based upon the bias curve of the 490 pixel high resolution camera displayed in Figure 2 the operating point was chosen to be 32 mV for a 3-fold neighbor coincidence, which corresponds to a pixel

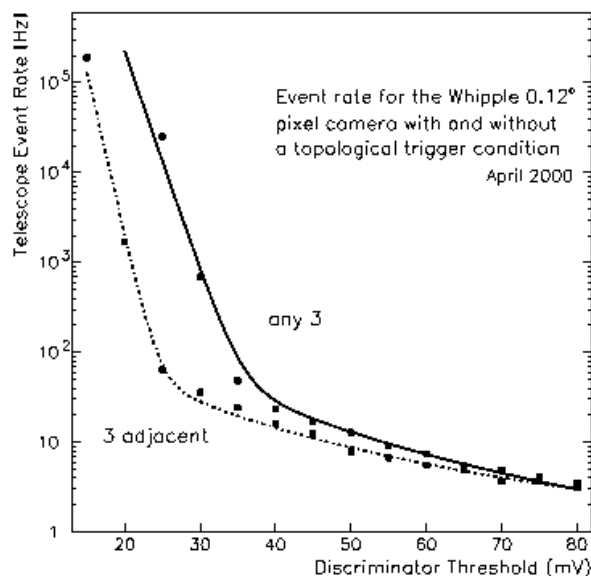


Fig. 2. A bias curve for the Whipple 10m telescope showing event rates for a simple multiplicity trigger (upper curve) and a 3-fold adjacent trigger from the hardware pattern selection trigger (lower curve). The steep part of the curves are due to accidental night sky coincidences while the flat part of the curve is a result of cosmic ray initiated events. The hardware pixel threshold was set at 32 mV based on the displayed data.

threshold of ~ 8 -10 photoelectrons.

Prior to analysis of the data the images are first flat-fielded and cleaned. The flat-fielding utilizes a Nitrogen arc lamp which illuminates the focal plane uniformly and allows for normalization of the PMT response on a nightly basis. The cleaning procedure relies upon determining the contribution of the night sky background to the signal in each channel. This is achieved by artificially triggering the system once per second and subsequently measuring the pedestal distribution resulting from these triggers in the charge-to-digital converters. In the analysis a pixel is considered a "picture" element if the signal it contains is greater than a predetermined picture threshold and a "boundary" element if the signal it contains is greater than a predetermined boundary threshold and it is adjacent to a picture element. All pixels not satisfying the picture and boundary criteria are zeroed. The picture and boundary thresholds for the 1999–2000 data were determined, by optimization, to be 4.25 and 2.25 times the standard deviation of the pedestal distribution for the channel while in 2001 the picture and boundary thresholds were determined, by optimization, to be 5.0 and 2.5 times the standard deviation of the pedestal distribution for the channel. A detailed discussion of the procedures outlined above can be found in Reynolds et al. (1993).

The Crab Nebula data, after flat-fielding and cleaning, is used to find an optimal set of data selection parameters based on the significance of the detected gamma-ray signal. The procedure is to vary one of the data selection parameters in-

dependently until the significance is optimized and then to set the parameter to its optimal value and vary the next parameter. After this optimization procedure is completed for all the selection parameters it is repeated to check for any correlated changes (the parameters are for the most part uncorrelated). Finally, an independent data sample is analyzed with the optimized set of data selection parameters to check for consistency and stability. The data selection parameters are jointly referred to as Supercuts and are essentially the moments of the light distribution for an individual event. The parameters are based upon simulations of extensive air showers produced by cosmic rays and gamma-rays and are discussed extensively in the literature (see e.g. Vacanti et al. (1991) and references therein). Briefly, the data selection parameters are based upon the total amount of detected light in the image (Size), the shape of the light distribution (Length and Width), the impact parameter of the event (Distance), and the orientation of the event (α). In addition there is also a selection on a parameter (Length/Size) intended to reduce the large background due to single muon events at low energies. Table 1 lists the optimized parameters for 3 recent epochs of the 10m telescope; the 331 pixel large field-of-view camera (1997–1999), the 490 pixel high resolution camera (1999–2000) prior to completion of the mirror recoating, and the 490 pixel camera (2000–2001) after completion of the GRANITE III upgrade.

The performance of the 10m telescope can then be evaluated in terms of the detected Crab Nebula gamma-ray rate. The Crab Nebula rates for the 3 epochs of the GRANITE III upgrade, 331 pixel large field-of-view camera, 490 pixel high resolution camera, and the 490 pixel high resolution camera upon completion of the upgrade, are displayed in Figure 3 and the details are tabulated in Table 2. This data comprises all Crab Nebula data taken during the relevant period with the exception of any data used in the optimization procedures described above. The high resolution camera, with the smaller pixel size relative to the 331 large field-of-view camera, allowed for better reconstruction of smaller images and thus resulted in a lower peak energy response for the 10m telescope. Upon completion of the mirror recoating and optimization of the picture and boundary thresholds described above the 10m telescope operated at its highest sensitivity ever. The peak energy response to a Crab-like spectrum¹ for the 3 epochs discussed here are: a) 500 ± 100 GeV for the 331 pixel camera, b) 430 ± 80 GeV, and c) 390 ± 80 GeV. The high resolution camera still has good response down to ≈ 200 GeV and is the primary reason for the increase in rate for the Crab Nebula given in Table 2.

4 Summary and Conclusions

The GRANITE III upgrade of the Whipple observatory 10m telescope was carried out in multiple phases over the period

¹The differential Crab Nebula flux is $J_{Crab} = (3.2 \pm 0.6) \times 10^{-7} (E/\text{TeV})^{-2.49 \pm 0.06} \text{ m}^{-2} \text{ s}^{-1} \text{ TeV}^{-1}$ (Hillas et al., 1998)

1997–2000. The completion of the upgrade in 2000 has led to the highest sensitivity that the 10m telescope has ever operated at. The high resolution camera has clearly demonstrated the utility of small pixels for better characterization of the gamma-ray and cosmic ray initiated air showers and the subsequent discrimination between the two that it leads to. The 2001 observing season, the first with the completely upgraded system, has yielded a rich data sample on the well established TeV AGN Mrk 421 (Holder, 2001) and a new detection of an extreme high energy BILac, 1H1426+428 (Horan, 2001). The successful GRANITE III upgrade has pointed the way to the rich scientific rewards that the completed VERITAS array, with its small pixel, large field-of-view cameras operating in a stereo mode, will yield.

Acknowledgements. The authors would like to thank K. Harris, E. Roache and the Whipple Observatory support staff for their technical assistance. The VERITAS Collaboration is supported by the U.S. Dept. of Energy, N.S.F., the Smithsonian Institution, P.P.A.R.C. (U.K.) and Enterprise-Ireland.

References

- Catanese, Michael, and Weekes, Trevor C., *PASP* 111, 1193–1222, 1999.
 Badran, H., *these proceedings*, 2001.
 S. M. Bradbury and H. J. Rose, *NIM*, *in the press*, 2001.
 De La Calle Perez et al., *these proceedings*, 2001.
 J.P. Finley et al., *B. L. Dingus, M. H. Salamon, and D. B. Kieda (eds.) Towards a Major Atmospheric Cherenkov Detector VI*, AIP Press, pgs. 301–307, 2000.
 Hillas, A. M. et al., *ApJ*, 503, 744–759, 1998.
 Horan, D., *these proceedings*, 2001.
 Holder, J., *these proceedings*, 2001.
 Reynolds, P. T., et al., *ApJ*, 404, 206–218, 1993.
 Vacanti, G. et al., *ApJ*, 377, 467–479, 1991.
 Weekes, T. C. et al., *ApJ* 342, 379–395, 1989.

Table 1: Supercuts

Parameter	1997–1999 331 pixel ^a	1999–2000 490 pixel ^b	2000–2001 490 pixel ^c
Total Size (dc ^d)	>400	N/A	N/A
Size ^e (dc)	100	30	50
Size ^f (dc)	80	30	40
Length	0°.16–0°.30	0°.13–0°.25	0°.09–0°.26
Width	0°.073–0°.15	0°.05–0°.12	0°.05–0°.13
Distance	0°.51–1°.10	0°.4–1°.0	0°.4–1°.0
Length/Size	N/A	<0.0004	<0.0004
α	<15°	<15°	<15°

^alarge field-of-view

^bhigh resolution

^cupgrade completed

^ddigital counts

^ebrightest image pixel

^fsecond brightest image pixel

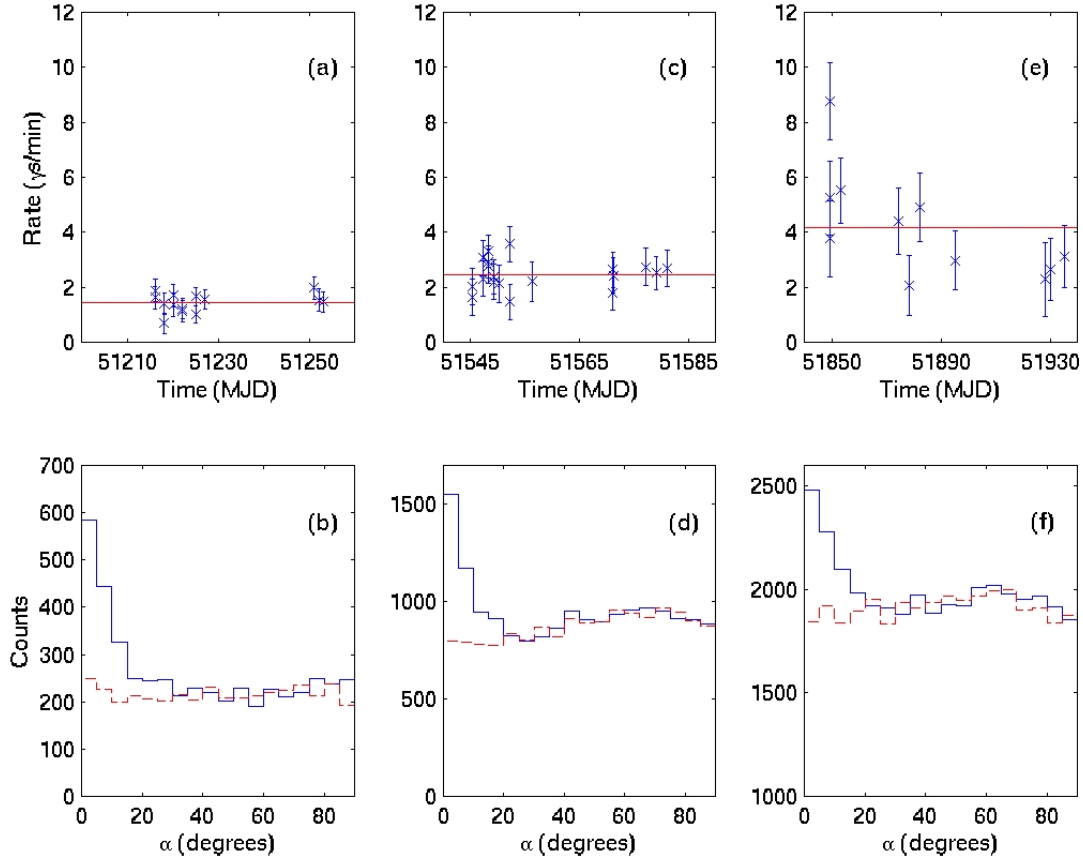


Fig. 3. Crab Nebula lightcurves and α distributions for the 331 pixel large field-of-view camera with Supercuts 1997 (left), the 490 pixel high resolution camera with Supercuts 2000 (middle), and the 490 pixel high resolution camera after completion of the GRANITE III upgrade using Supercuts 2001 (right). The mean rates are indicated by the red line in the lightcurves and the off-source α distributions are indicated by the dashed red line.

Table 2: Crab Nebula Data

	1997–1999 ^{ab}	1999–2000 ^c	2000–2001 ^d
Data Pairs ^e	14	19	11
Epoch (MJD)	51216–51253	51545–51581	51849–51884
Rate (γs/min)	1.44±0.35	2.46±0.15	4.15±0.39
Significance (σ)	14.02	16.70	11.17

^alarge field-of-view

^bpost hardware pattern selection trigger

^chigh resolution

^dupgrade completed

^ea data pair consists of a 28 minute on and off source run